

# 2 kHz High Power Smart Transducer for Acoustic Sub-bottom Profiling Applications

R. Sathishkumar\*

Electronics and Communication Engineering Department, KL University, Vijayawada 522502, India

**Abstract:** In this study, a 2 kHz Tonpilz projector was designed using a Terfenol-D and modeled in ATILA. For the purpose of modeling studies, it has been determined that a radiating head mass exhibits better transmitting current response (TCR) at 136 mm diameter, where the resonance occurs at 2.4 kHz and the peak value of 118 dB re 1  $\mu\text{Pa/A}$  at 1 m occurs at 12 kHz. Also bolt at a 46 mm distance from the center of the head mass offers resonance at 2.4 kHz, and the peak value of 115.3 dB re 1  $\mu\text{Pa/A}$  at 1 m occurs at 11.5 kHz. This optimized design is fabricated and molded with polyurethane of 3 mm thickness. The prototype was tested at the Acoustic Test Facility (ATF) of National Institute of Ocean Technology (NIOT) for its underwater performances. Based on the result, the fundamental resonance was determined to be 2.18 kHz and the peak value of TCR of 182 dB re 1  $\mu\text{Pa/A}$  at 1 m occurs at 14 kHz. The maximum value of the RS was found to be -190 dB re 1 V/ $\mu\text{Pa}$  at 1 m at a frequency of 2.1 kHz.

**Keywords:** smart transducer; magnetostriction; acoustic sub-bottom profiling; transmitting current response (TCR)

**Article ID:** 1671-9433(2013)03-0361-05

## 1 Introduction

Acoustic sub-bottom profiling application requires wide bandwidth, compact and effectively high-power low-frequency sources of sound (Lin, 2009). Commercial acoustic transducers are made of PZT material (Sherlock and Meyer, 2012a). The magnetostrictive transducers, physically vibrates at its resonant frequency that possesses the ability to generate broadband, and high force responses (Yang *et al.*, 2010; Evans and Dapino, 2011). These projectors are designed to produce 10 times higher power efficiency than the same size and weight of piezoelectric projectors. The transducer vibrations impart a periodic motion to the particles of the medium in contact with it, which constitutes the acoustic wave. Its sensitivity, radiation pattern and operating frequency also prescribes the information for signal processing. Advanced giant magnetostrictive materials (GMM) can be used to achieve a low weight, and small size acoustic projector delivering high powers compared to the conventional materials. Terfenol-D is a powerful smart material and its performance is reliable (Slaughter, 2011; Meng *et al.*, 2013).

## 2 Design of the Tonpilz transducer

The Tonpilz design produces reinforced mechanical motion of high power sound generation. Detailed discussion of these longitudinal vibrators is given in Slaughter *et al.* (2011). Sherlock and Meyer (2012b) show clearly the operation of tonpilz designs. It is typically made up of an active element  $E_A$  placed between a light alloy head mass  $M_H$  and a heavy tail mass  $M_T$ . This design is a series of mechanical arrangements of  $M_H$ , magnetic coupler  $C_M$ , AE, and  $M_T$ . The resonance of the combination is

$$\omega^2 = k \frac{M_H + M_T}{M_H \cdot M_T} \quad (1)$$

where  $k$  is the stiffness of the  $E_A$ , and  $\omega$  is the angular frequency. In general

$$k = \frac{YA}{l} \quad (2)$$

where  $Y$  is the Young's modulus  $= 4 \times 10^{10} \text{ N/m}^2$ ,  $A$  is the area of cross section  $= 70.6 \times 10^{-5} \text{ m}^2$ , and  $l$  is the length of the active material  $= 10 \times 10^{-2}$ . From the Table 1, the stiffness of the active material is calculated as  $k = 28.24 \times 10^7 \text{ N/m}$ . From the Eq. (1), the  $M_H$  and  $M_T$  are calculated as 780 g and 2340 g respectively to have a resonance frequency of 3 kHz in water. To get reasonably good radiation characteristics, the ratio of the area of the piston  $A_P$  and the area of the active material  $A_M$  is selected as 21. Based on these constraints, the diameter of the  $M_H$  is fixed as 136 mm. Further aluminum has been used as  $M_H$  and mild steel for  $M_T$  (due to its higher density). In the present work three 5 mm diameter stainless steel rods are used to give a prestress. The magnetostrictive material Terfenol-D rod, of 100 mm length and 30 mm diameter, has been selected as the  $E_A$ . The magnetic field outside the rod is minimized by making the dimensions of the  $C_M$  larger than the  $E_A$ . The linear output is obtained by the 50 mm diameter and 20 mm thickness Neodymium Iron Boron (NdFeB), a rare-earth permanent magnet that has high remanence and high coercive force that obtain the bias field. The AC is passed through solenoid to obtain oscillations that partially expand  $E_A$  into the middle of its linear strain region, minimizing electrical requirements and increasing sensitivity. The  $E_A$  needs to be biased at around 300 Oe for obtaining maximum coupling coefficient. The field generated by a solenoid is governed by the number of turns of the tuning

Received date: 2013-02-28.

Accepted date: 2013-05-27.

\*Corresponding author Email: drsathishkumar@gmail.com

© Harbin Engineering University and Springer-Verlag Berlin Heidelberg 2013

coil and the maximum current that can be sent through the coil.

$$H = \frac{4\pi}{10} nI \text{ Oe} \quad (3)$$

where  $n$  is the number of turns per centimeter and  $I$  is the current in the coil. Hence 700 turns of SWG18 copper wire are used to generate 270 Oe for a current of 3.1 A.

### 3 Modeling studies

The analysis of transducers by integrating Laplace equations (ATILA) is FEM software that can compute every shape of the complete transducer (Debus *et al.*, 2006; Harvey and Gachagan, 2011). The  $E_A$  properties used in the model are listed in Table 1 that compares PZT and Terfenol-D. The Fig. 1 illustrates the design steps involved in ATILA modeling and the geometry is shown in Fig. 2. The projector along with the fluid structure interaction has been modeled and the studies have been carried out by varying the dimensions of the  $M_H$  and the stress bolt at various locations. The water is used as fluid with compressibility of  $2.22 \times 10^9 \text{ N/m}^2$  and density of  $1000 \text{ kg/m}^3$ . The projector including the fluid has been divided into 2019 elements. The structural and fluid elements are 295 and 318, respectively, and 16 elements are interfacing elements between the solid structure and the fluid. Also 28 elements are damping elements representing radiation condition. The Figs. 3, 4 show the mesh generated and the displacement. The Fig. 5 shows the comparison of the transmitting current response (TCR) for various  $M_H$  diameters. From the figure, at 136 mm it shows the better performance, where the fundamental resonance occurs at 2.4 kHz and the peak value of 118 dB re  $1 \mu\text{Pa/A}$  at 1m occurs at 12 kHz. The comparison of TCR for the bolts at various distances is shown Fig. 6. From the figure, at a 46 mm distance from the center of the  $M_H$  it offers the better results, where the fundamental resonance occurs at 2.4 kHz and the peak value of 115.3 dB re  $1 \mu\text{Pa/A}$  at 1m occurs at 11.5 kHz.

**Table 1 Comparison of Terfenol-D and PZT**

Property	PZT	Terfenol-D
Maximum strain ( $\times 10^{-6}$ )	100–300	1400–2000
Coupling factor/( $\text{kg} \cdot \text{m}^{-3}$ )	0.65	0.7–0.8
Density	7500	9150
Young's modulus/( $\text{N} \cdot \text{m}^{-2}$ )	$7.3 \times 10^{10}$	$4 \times 10^{10}$
Sound speed/( $\text{m} \cdot \text{s}^{-1}$ )	3400	1800–2500
Electromechanical energy density/( $\text{J} \cdot \text{m}^{-3}$ )	670	14000–25000
Specific acoustic impedance/rayls	$2.6 \times 10^7$	$2.2 \times 10^7$



**Fig. 1 ATILA design process**

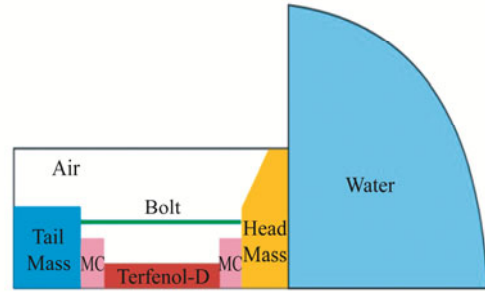


**Fig. 2 Geometry of the transducer**

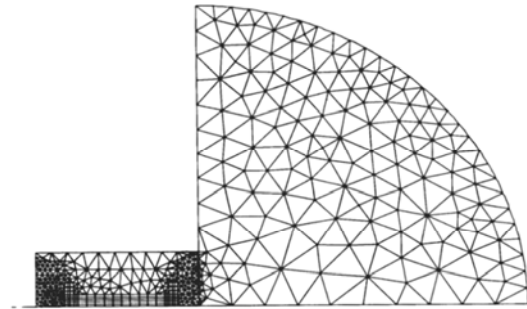


**Fig. 3 Mesh used for ATILA computation**

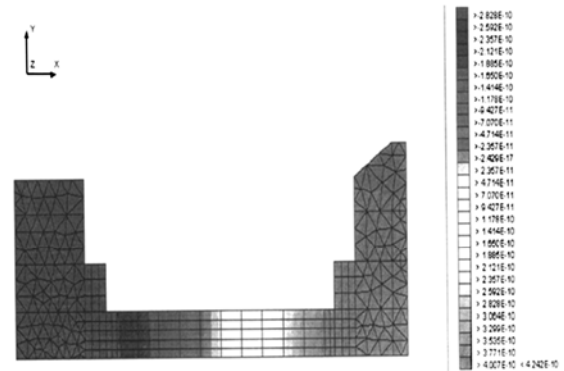


**Fig. 4 Displacement of the projector**

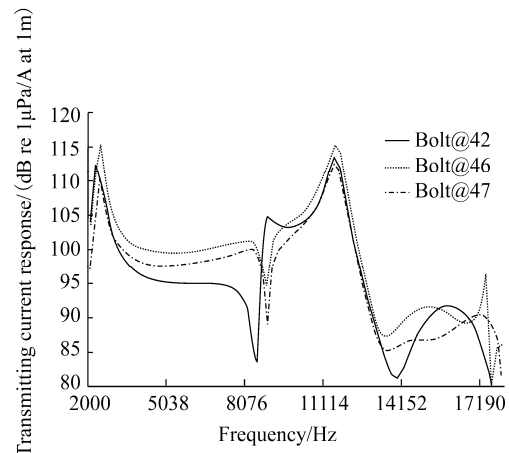


**Fig. 5 Comparison of TCR for various  $M_H$  diameters**

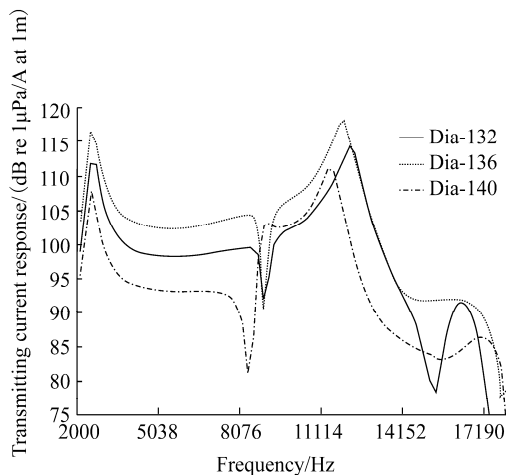


Fig. 6 Comparison of Bolt at different locations

#### 4 Fabrication

The prototype has been built on the basis of the optimized design ( $M_H$  is 136 mm and bolt is at a 46 mm distance from the center of  $M_H$ ) as shown in Fig. 7. The steel bolt is used to maintain a preload and is fixed in an enclosure to protect from exposure to water. The casing is made out of marine grade aluminum IS 5500, which has high mechanical properties (ultimate tensile strength is 244.9 N/mm<sup>2</sup> and yield strength is 122.5 N/mm<sup>2</sup>) with good impact strength and better corrosion resistance. The  $M_H$  is molded using polyurethane with 3 mm thickness, which protects the metal masses from corrosion and maintaining the transparency to acoustic radiations.

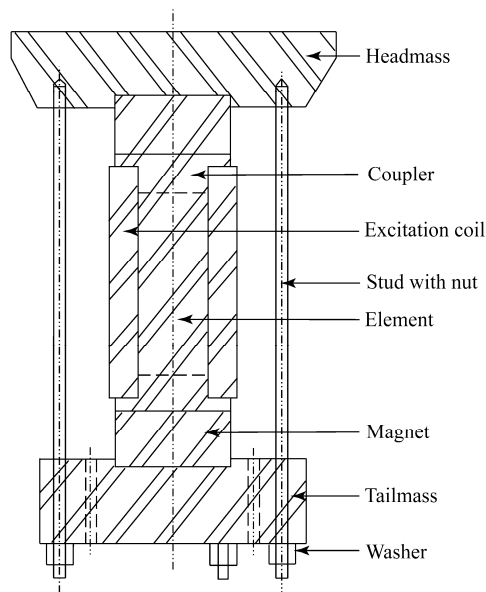


Fig. 7 Element assembly

#### 5 Testing and results

The acoustical measurements were conducted at the

Acoustic Test Facility (ATF) of National Institute of Ocean Technology (NIOT) at an ambient temperature of 26°C and a water temperature of 28.8°C. The distance between projector and receiver is 4.5 m and the depth is 3 m. The measured in-water electrical power and impedance are given in Tables 2 and 3. The TCR was measured in the frequency range of 2 kHz to 16 kHz, as shown in Fig. 8, where the fundamental resonance is seen to be 2.18 kHz and the peak value of TCR is 182 dB re 1 μP/A at 1 m occur at 14 kHz. The maximum value of the receiving sensitivity (RS) was found to be -190 dB re 1 V/μPa at 1 m a frequency of 2.1 kHz as shown in Fig. 9. The transmitting directivity pattern was obtained at a frequency of 4 kHz, 7 kHz in steps of 1° and the typical response is shown in Fig. 10. The maximum power handled by the transducer is 1 490 W (RMS).

Table 2 Electrical impedance

Frequency/Hz	Magnitude (in water)	Magnitude (in air)
1 500	68.114	70.033
2 500	94.331	94.815
3 500	123.425	125.270
4 500	149.245	151.087
5 500	178.392	179.588
6 500	203.815	205.784
7 500	229.094	232.277
8 500	252.194	257.822
9 500	279.647	286.026
10 500	293.416	290.589
11 500	325.490	331.139
12 500	357.153	360.874
13 500	380.164	378.317
14 500	383.457	408.958
15 500	423.531	420.148
16 500	443.443	464.343
17 500	473.937	490.973
18 000	448.233	503.055

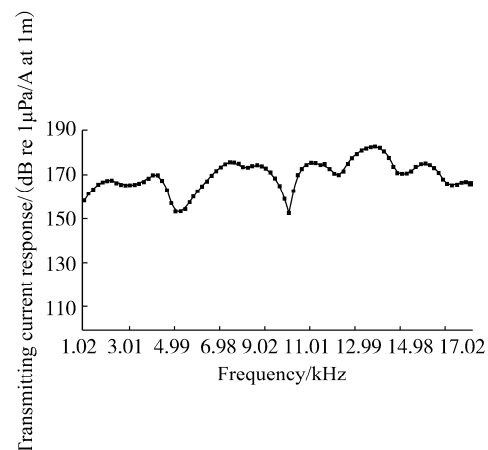


Fig. 8 TCR of the prototype transducer

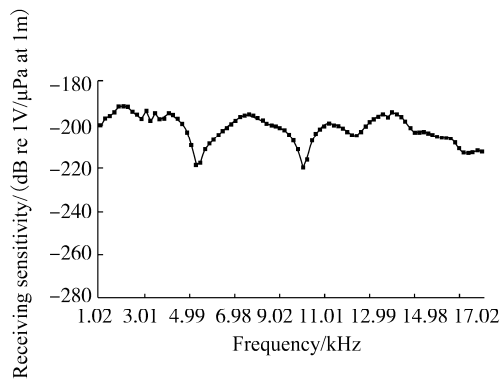


Fig. 9 RS of the prototype transducer

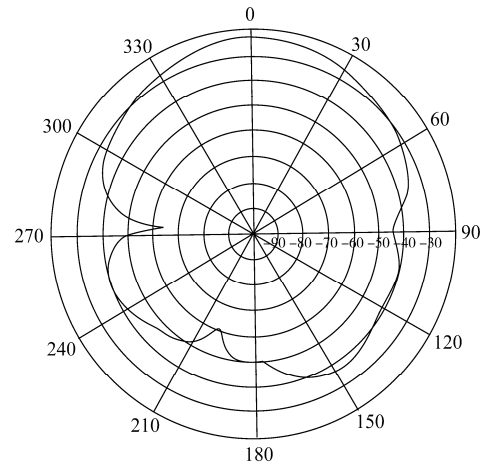


Fig. 10 Beam pattern of the prototype projector

Table 3 Electrical power

Frequency /kHz	Power/W (RMS)	Transmitted current/A (RMS)	Transmitted voltage/V (RMS)	Phase/(°)	$V(\%)$ distortion	$I(\%)$ distortion
3.5	429	1.52	212.16	67.0	3.14	25.70
	547	1.67	239.04	66.0	3.90	26.00
	667	1.87	265.21	66.0	3.00	21.40
	834	2.11	291.37	66.0	2.96	17.90
	946	2.24	307.64	64.2	2.90	20.80
3.5	990	2.29	318.74	68.9	2.40	17.00
	472	1.25	329.56	69.0	1.60	17.60
	587	1.37	366.34	66.0	1.10	14.70
	850	1.70	439.18	69.0	1.30	16.00
	1040	1.87	473.83	67.0	1.40	12.00
14.0	1170	2.02	512.02	64.0	1.30	11.00
	1293	2.16	534.65	61.0	1.30	9.50
	1490	2.27	571.43	66.0	1.02	10.30
	846	1.27	554.46	61.2	0.99	8.50
	961	1.39	599.72	65.0	1.14	10.10
14.0	1040	1.52	644.27	62.3	1.20	9.00
	1270	1.68	648.51	61.5	1.20	9.70
	1330	1.72	714.29	68.9	1.50	6.00
	1440	1.79	742.57	68.3	1.40	6.00

## 5 Conclusions

A broadband Tonpilz transducer was designed, modeled, fabricated and tested for a marine application. The experimental measurements agreed with the model results; and ATILA, the TCR resonance occurs at 2.4 kHz, whereas in prototype it occurs at 2.18 kHz. The measured and predicted resonances were determined to be within 2.5 kHz. Further, in the modeling results, the dips were observed around 9 kHz and 13.5 kHz respectively. But in prototype the dips were observed around 4.9 kHz and 9.9 kHz. The projector allowed for RS and the behavior of the curve was found to be similar to that of the TCR. The reason for the sharp dips in TCR/RS plots need to be studied further. Several possible factors (mechanical losses and difference between the real material data and data used in the calculations) could result in the deviation. The bandwidth

can be improved to a limited extent by reducing the thickness or increasing the diameter of  $M_H$ . The fundamental resonance and the desired usable frequency band can also be tailored. It shows a broadband behavior as per expectations but the performance needs to be improved to get a broadband without the dips for using it in future marine applications. The vibration mode in relation to the prestress bolt of the projector is another potential mode, which can be used to improve the bandwidth further. This approach is currently being investigated, and the results of an improved model will be reported in the future.

## Acknowledgement

I am grateful to the director of National Institute of Ocean Technology–NIOT, for providing the necessary facilities for the present work. I received a lot of guidance, continual encouragement and support from Dr. Dhilsha Rajappan,

joint project director of NIOT, who provided us the initial desire, interest and ideas on ocean engineering projects.

## References

- Debus JC, Blottman J, Butler S (2006). Thermal behavior of high-power active devices with the ATILA finite-element code. *Journal of Acoustical Society of America*, **120**(5), 3274-3274.
- Evans PG, Dapino MJ (2011). Dynamic model for 3-D magnetostrictive transducers. *IEEE Transactions on Magnetics*, **47**(1), 221-230.
- Harvey G, Gachagan A (2011). Simulation and measurement of nonlinear behavior in a high-power test cell. *IEEE Transactions on Ultrasonics, Ferroelectrics and Frequency Control*, **58**(4), 808-819.
- Lin Shuyu (2009). Analysis of multi frequency langevin composite ultrasonic transducers. *IEEE Transactions on Ultrasonics, Ferroelectrics and Frequency Control*, **56**(9), 1990-1998.
- Meng Aihua, Zhu Jiaming, Kong Min, He Hanlin (2013). Modeling of Terfenol-D biased minor hysteresis loops. *IEEE Transactions on Magnetics*, **49**(1), 552-557.
- Sherlock NP, Meyer RJ (2012a). Electromechanical nonlinearities and losses in piezoelectric sonar transducer materials. *IEEE Transactions on Ultrasonics, Ferroelectrics and Frequency Control*, **59**(8), 1618-1623.
- Sherlock NP, Meyer RJ (2012b). Modified single crystals for high-power underwater projectors. *IEEE Transactions on Ultrasonics, Ferroelectrics and Frequency Control*, **59**(6), 1285-1291.
- Slaughter JC (2011). A compact Terfenol-D vector projector. *Journal of Acoustic Society of America*, **130**(4), 2505-2505.
- Yang Jin, Wen Yumei, Li Ping, Dai Xianzhi, Li Ming (2010). A broadband vibration energy harvester using magnetoelectric transducer. *IEEE Sensors*, Kona, 1905-1909.

## Author biography



**R. Sathishkumar** is presently a professor of Electronics and Communication Engineering, School of Electrical Sciences of KL University, India. He has involved in the Ocean Engineering research work regarding the design and optimization of Sonar systems. His activities are documented by an extensive publication record of scientific research articles, technical reports, and papers at international proceedings (over 30 publications stand June 2013). He was awarded as 'Outstanding Scientist' in 2012 by NFED, India. He received various prize awards for his overall research work and his scientific contributions to Signal and Image processing of sonar systems.